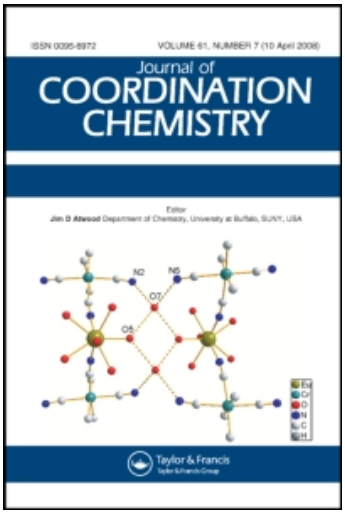

**Journal of Coordination Chemistry**
Publication details, including instructions for authors and subscription information:
http://www.informaworld.com/smpp/title~content=t713455674

# Syntheses, structures, and properties of two new hybrid Dawson-based polyoxotungstates $[Mn(2,2'\text{-bipy})_3]H_2$ $[Mn(2,2'\text{-bipy})_2][P_2W_{18}O_{62}]$ and $[Co(H_2biim)_3)]_2H_2[P_2W_{18}O_{62}] \cdot 8H_2O$

Qiang Wu[ab]; Xiao Fu[a]; Junwei Zhao[a]; Suzhi Li[a]; Jingping Wang[a]; Jingyang Niu[a]
[a] Institute of Molecular and Crystal Engineering, College of Chemistry and Chemical Engineering, Henan University, Kaifeng, Henan 475004, P.R. China [b] Pharmaceutical College, Henan University, Kaifeng, Henan 475004, P.R. China

First published on: 25 June 2010

**To cite this Article** Wu, Qiang , Fu, Xiao , Zhao, Junwei , Li, Suzhi , Wang, Jingping and Niu, Jingyang(2010) 'Syntheses, structures, and properties of two new hybrid Dawson-based polyoxotungstates $[Mn(2,2'\text{-bipy})_3]H_2$ $[Mn(2,2'\text{-bipy})_2][P_2W_{18}O_{62}]$ and $[Co(H_2biim)_3)]_2H_2[P_2W_{18}O_{62}] \cdot 8H_2O$', Journal of Coordination Chemistry, 63: 11, 1844 — 1855, First published on: 25 June 2010 (iFirst)
**To link to this Article: DOI:** 10.1080/00958972.2010.495773
**URL:** http://dx.doi.org/10.1080/00958972.2010.495773

*Journal of Coordination Chemistry*
Vol. 63, No. 11, 10 June 2010, 1844–1855



# Syntheses, structures, and properties of two new hybrid Dawson-based polyoxotungstates $[Mn(2,2'\text{-bipy})_3]H_2$ $[Mn(2,2'\text{-bipy})_2][P_2W_{18}O_{62}]$ and $[Co(H_2biim)_3)]_2H_2[P_2W_{18}O_{62}] \cdot 8H_2O$

QIANG WU†‡, XIAO FU†, JUNWEI ZHAO†, SUZHI LI†, JINGPING WANG† and JINGYANG NIU*†

†Institute of Molecular and Crystal Engineering, College of Chemistry and Chemical Engineering, Henan University, Kaifeng, Henan 475004, P.R. China
‡Pharmaceutical College, Henan University, Kaifeng, Henan 475004, P.R. China



(*Received 15 November 2009; in final form 3 February 2010*)

Two new hybrid Dawson-based polyoxotungstates, $[Mn(2,2'\text{-bipy})_3]H_2[Mn(2,2'\text{-bipy})_2][P_2W_{18}O_{62}]$ (**1**) and $[Co(H_2biim)_3)]_2H_2[P_2W_{18}O_{62}] \cdot 8H_2O$ (**2**) (2,2′-bipy = 2,2′-bipyridine, $H_2biim$ = 2,2′-biimdazole), have been prepared under hydrothermal conditions and characterized by single-crystal X-ray diffraction, elemental analyses, IR spectra, thermogravimetric analyses (TGA), X-ray photoelectron spectroscopy (XPS), and photoluminescence spectra. Compound **1** is a 1-D zigzag chain constructed from alternate Dawson-type heteropolyanions $[\alpha\text{-}P_2W_{18}O_{62}]^{6-}$ and metal coordination cations $[Mn(2,2'\text{-bipy})_2]^{2+}$, in which the 1-D chains are extended into a 3-D framework through C–H $\cdots\pi$ and $\pi$–$\pi$ stacking interactions. Compound **2** is a discrete structure consisting of $[\alpha\text{-}P_2W_{18}O_{62}]^{6-}$ and two $[Co(H_2biim)_3)]^{2+}$ cations, forming a 3-D supramolecular framework *via* N–H $\cdots$ O hydrogen bonds and C–H $\cdots\pi$ interactions. Photoluminescence properties of **1** and **2** have been investigated at room temperature.

*Keywords*: Polyoxometalates; Biimdazole; Polyoxotungstate; Dawson structure

## 1. Introduction

Organic–inorganic hybrid compounds have been attracting considerable interest owing to their fascinating solid state structures and potential applications in catalysis, medicine, biology, and material science [1–4]. Polyoxometalates (POMs), as an important family of metal oxide with general formula $[X_xM_mO_y]^{n-}$ (X = Si, P, B, Co, As, etc.; M = Mo, W, V, Nb, etc.), have been widely used as inorganic materials because of their variety of components, molecular characteristics, properties, and applications [5–7]. Keggin, Dawson, Lindquist, and Anderson classical POM structural types have been employed as inorganic building blocks to construct 0-, 1-, 2-, and 3-D organic–inorganic hybrid materials by incorporating metal–organic complexes into the inorganic POM systems [8–12]. In POM chemistry, compared with saturated

*Corresponding author. Email: jyniu@henu.edu.cn

*Journal of Coordination Chemistry*
ISSN 0095-8972 print/ISSN 1029-0389 online © 2010 Taylor & Francis
DOI: 10.1080/00958972.2010.495773

Keggin-type and Anderson-type polyoxotungstates, reports on hybrid Dawson-based polyoxotungstates are comparatively rare [13–20].

In 2004, we reported two 0-D organic–inorganic hybrid Dawson-type POM lanthanide derivatives $[Gd(DMF)_6(H_2O)_2]_2[P_2W_{18}O_{62}]\cdot 4DMF\cdot 2H_2O$ and $[Ce(NMP)_3(H_2O)_5][Ce(NMP)_3(H_2O)_4][(P_2W_{18}O_{62})]\cdot 4H_2O$ [13a]. In 2007, Wang's and Peng's group described several new 0-D Dawson-type POMs $[Cu^{II}(en)(2,2'\text{-bipy})]_3[P_2W_{18}O_{62}]\cdot 3H_2O$ [14], $[Cu(2,2'\text{-bipy})_3]_2[Cu(2,2'\text{-bipy})_2]_2[P_2W_{18}O_{62}]$, and $[2,2'\text{-bipy}]_8[Fe(2,2'\text{-bipy})_3]_8[P_2W_{18}O_{62}]_4\cdot 9H_2O$ [15]. Since 2004, our group has prepared a family of 1-D chain architectures from Dawson-type polyanions and rare earth coordination cations, $[\{Gd(DMF)_6\}\{Gd(DMF)_7\}(P_2W_{18}O_{62})]\cdot 0.5DMF$ [13a], $[\{Ce(DMF)_4(H_2O)_3\}\{Ce(DMF)_4(H_2O)_4\}(P_2W_{18}O_{62})]\cdot H_2O$ [13b], $[\{La(DMF)_6(H_2O)\}\{La(DMF)_{4.5}(H_2O)_{2.5}\}(P_2W_{18}O_{62})]$ [13b], and $H_{1.5}[Sm(H_2O)_8]_{0.5}[Sm(DMF)_6(H_2O)(\alpha\text{-}P_2W_{18}O_{62})]\cdot DMF\cdot 3H_2O$ [13c]. Furthermore, organic–inorganic hybrid Dawson-type POM transition metal derivatives were also reported, such as $[\{Cu_2(2,4'\text{-Hbpy})_4\}Mo_{18}As_2O_{62}]\cdot 2H_2O$ [16], $[HenMe]_2[Cu(enMe)_2][\{Cu(enMe)_2\}P_2W_{18}O_{61}]\cdot 9H_2O$ (enMe = 1,2-diaminopropane) [17], $[M(phen)_2(H_2O)_2][\{M(phen)_2\}\{M(phen)_2(H_2O)_x\}\{P_2W_{18}O_{62}\}]\cdot nH_2O$ {[M = Zn, Cd] (X = 1,3)} [18], and $(H_3btb)[Fe(btb)_3(P_2W_{18}O_{62})]\cdot 4H_2O$ (phen = 1,10′-phenanthroline, btb = 1,4-bis(1,2,4-triazol-1-y1)butane) [19]. The above-mentioned Dawson-type POM transition metal derivatives are all 1-D chains built by Dawson-type polyoxoanions and transition-metal complexes through terminal oxygens located in "belt" sites of Dawson polyanions rather than "cap" sites. The first 2-D Dawson-type POM $(NH_4)_3(4,4'\text{-}H_2bipy)[Cu^{I}(4,4'\text{-bipy})]_7[P_2W_{18}O_{62}]_2\cdot 10H_2O$ was isolated by Wang *et al.* [14] in 2007, in which $[P_2W_{18}O_{62}]^{6-}$ clusters are linked by $\{Cu(4,4'\text{-bipy})\}_n^{n+}$ chains. Subsequently, Yang *et al.* [20] discovered another 2-D (4,4)-connected topological network $[4,4'\text{-}H_2bipy]_2\{[Cu(4,4'\text{-bipy})_3][Cu(4,4'\text{-bipy})_4(H_2O)_2]_2[Cu(4,4'\text{-bipy})][\alpha\text{-}P_2W_{18}O_{62}]_2\}\cdot 6H_2O$. Recently, Peng *et al.* [21] obtained the first 3-D Dawson-type framework $[Cu(4,4'\text{-bipy})]_2[H_4P_2W_{18}O_{62}]\cdot 2H_2O$. Later, they reported a series of 3-D hybrid compounds constructed from Dawson polyoxoanion and silver complexes, $\{[Ag(bipy)]_2[P_2W_{18}O_{62}]\}2[H_2bipy]\cdot 4H_2O$ [22a], $[\{Ag(H_2O)(phnz)\}\{Ag(phnz)\}_5(P_2W_{18}O_{62})][phnz]_{0.5}\cdot 4H_2O$ [22b], $\{[Ag(bipy)]_4[P_2W_{18}O_{62}]\}\cdot 2[Hbipy]$ [22a] and $[Ag(bipy)]_2[Ag(bipy)(Hbipy)][P_2W_{18}O_{62}]\cdot[H_2bipy]$ (bipy = 4,4′-bipyridine, phnz = phenazine) [22c]. In 2008, our group reported a new example of 3-D framework $H_2[Ca_2(P_2W_{18}O_{62})(H_2O)_5]\cdot 7.5H_2O$ based on Dawson anions and calcium cations [23]. Liu *et al.* [24] addressed two Dawson-templated 3-D metal–organic frameworks $[M_2(bipy)_3(H_2O)_2(ox)][P_2W_{18}O_{62}]\cdot 2(H_2bipy)\cdot nH_2O$ (M = Co(II), $n = 3$; M = Ni(II), $n = 2$) (bipy = 4,4′-bipyridine; $ox = C_2O_4^{2-}$). Another hybrid Dawson-type POM dimer $[Hen][Cu(en)_2(H_2O)]_2[Cu(en)_2(H_2O)_2]_{0.5}[\{Cu(en)_2(H_2O)\}_2\{Cu(en)_2\}(P_2W_{18}O_{61})_2]\cdot en\cdot nH_2O$ separated by Lin *et al.* [17] consists of two Wells–Dawson units bridged by a $[Cu(en)]^{2+}$ cation.

Hydrothermal method is an effective strategy in preparing multidimensional structures with interesting properties [14–16, 25]. Here, we employ hydrothermal reaction of $\alpha\text{-}H_6P_2W_{18}O_{62}\cdot nH_2O$, 2,2′-bipy/$H_2$biim (2,2′-bipy = 2,2′-bipyridine, $H_2$biim = 2,2′-biimdazole) with transition metals to construct Dawson-based polyoxotungstates with extended structures. We have isolated two new hybrid Dawson-based polyoxotungstates $[Mn(2,2'\text{-bipy})_3]H_2[Mn(2,2'\text{-bipy})_2][P_2W_{18}O_{62}]$ (**1**) and $[Co(H_2biim)_3)]_2H_2[P_2W_{18}O_{62}]\cdot 8H_2O$ (**2**). Both have been characterized by single-crystal X-ray diffraction, elemental analyses, infrared (IR) spectra, thermogravimetric analyses (TGA), X-ray photoelectron spectroscopy (XPS), and photoluminescence

spectra. Compound **1** has a 1-D zigzag chain constructed from alternate Dawson-type heteropolyanions $[\alpha\text{-}P_2W_{18}O_{62}]^{6-}$ and $[Mn(2,2'\text{-bipy})_2]^{2+}$; the 1-D chains are extended into a 3-D framework through C–H $\cdots\pi$ and $\pi$–$\pi$ stacking interactions. Compound **2** is a discrete structure consisting of $[\alpha\text{-}P_2W_{18}O_{62}]^{6-}$ and two $[Co(H_2biim)_3)]^{2+}$, forming a 3-D supramolecular framework *via* N–H $\cdots$ O hydrogen bonds, C–H $\cdots\pi$ and electrostatic interactions. Photoluminescence properties of **1** and **2** have been investigated at room temperature.

## 2. Experimental

### 2.1. *Physical measurements and materials*

All chemicals are reagent grade and used as received from commercial sources. $\alpha\text{-}H_6P_2W_{18}O_{62}\cdot nH_2O$ was prepared according to the literature method and verified by IR spectrum [26]. C, H, and N elemental analyses were performed on a Perkin Elmer 240C elemental analyzer. IR spectra were recorded on a Nicolet 170 SXFT-IR spectrometer using KBr pellets from 400 to 4000 $cm^{-1}$. TGA measurements were carried out on a Perkin Elmer 7 thermal analyzer in flowing $N_2$ at a heating rate of 10°C $min^{-1}$. XPS analyses were performed on an AXIS ULTRA spectrometer with an Al-K$\alpha$ achromatic X-ray source. Emission/excitation spectra were recorded on a F-7000 fluorescence spectrophotometer.



### 2.2. *Preparation of [Mn(2,2′-bipy)$_3$]H$_2$[Mn(2,2′-bipy)$_2$][P$_2$W$_{18}$O$_{62}$] (1)*

A mixture of $MnCl_2\cdot 4H_2O$ (0.08 g, 0.4 mmol), $\alpha\text{-}H_6P_2W_{18}O_{62}\cdot nH_2O$ (0.42 g, 0.29 mmol), 2,2′-bipy (0.04 g, 0.4 mmol), triethylamine (trea) (0.1 mmol) and $H_2O$ (10 mL) was stirred for 1 h in air and the pH adjusted to 5.4 with 0.5 mol $L^{-1}$ KOH. The resulting mixture was transferred to a Teflon-lined stainless steel autoclave (20 mL) and kept at 170°C for 6 days. After the autoclave cooled to room temperature, red block-shaped crystals of **1** were filtered off, washed with distilled water, and air-dried to give a yield of 0.231 g (yield 55% based on 2,2′-bipy). Anal. Calcd (found) for **1** (wt.%): C: 11.43% (11.58%); H: 8.05% (7.96%); N: 2.66% (2.75%).

### 2.3. *Preparation of [Co(H$_2$biim)$_3$)]$_2$H$_2$[P$_2$W$_{18}$O$_{62}$]·8H$_2$O (2)*

A mixture of $CoCl_2\cdot 6H_2O$ (0.07 g, 0.29 mmol), $\alpha\text{-}H_6P_2W_{18}O_{62}\cdot nH_2O$ (0.42 g, 0.29 mmol), 2,2′-biimidazole ($H_2biim$) (0.09 g, 0.67 mmol), triethylamine (trea) (0.1 mmol), and $H_2O$ (9 mL) was stirred for 1 h in air and the pH adjusted to 5.6 with 0.5 mol $L^{-1}$ KOH. The mixture was transferred to a Teflon-lined stainless steel autoclave (20 mL) and kept at 170°C for 6 days. After the autoclave cooled to room temperature, orange block-shaped crystals of **2** were filtered off, washed with distilled water, and air-dried to give a yield of 0.364 g (yield 46% based on $CoCl_2\cdot 6H_2O$). Anal. Calcd (found) for **2** (wt.%): C: 8.01% (8.15%); H: 0.93% (1.07%); N: 6.23% (6.41%).

Table 1. Crystallographic data and structural refinements of **1** and **2**.

| | **1** | **2** |
|---|---|---|
| Empirical formula | $C_{50}H_{42}Mn_2N_{10}O_{62}P_2W_{18}$ | $C_{36}H_{54}Co_2N_{24}O_{70}P_2W_{18}$ |
| Formula weight | 5255.84 | 5431.87 |
| Temperature (K) | 296(2) | 296(2) |
| Wavelength (Å) | 0.71073 | 0.71073 |
| Crystal system | Monoclinic | Monoclinic |
| Space group | *P 2(1)/n* | *P 2(1)/c* |
| Unit cell dimensions (Å, °) | | |
| *a* | 16.1328(14) | 12.7923(13) |
| *b* | 21.1721(18) | 50.705(5) |
| *c* | 31.700(3) | 14.8945(16 |
| *β* | 98.852(2) | 90.213(2) |
| Volume (Å$^3$), *Z* | 10,698.7(16), 4 | 9661.0(17), 4 |
| Calculated density (g cm$^{-3}$) | 3.261 | 3.733 |
| Absorption coefficient (mm$^{-1}$) | 19.609 | 21.813 |
| *F*(000) | 9264 | 9648 |
| *θ* range for data collection (°) | 1.62–25.00 | 0.80–25.00 |
| Limiting indices | $-19 \le h \le 19$; $25 \le k \le 23$; $-35 \le l \le 37$ | $-14 \le h \le 15$; $-48 \le k \le 60$; $-14 \le l \le 17$ |
| Reflections collected | 52897 | 49660 |
| Independent reflection | 18,597 [$R$(int) = 0.0909] | 17,005 [$R$(int) = 0.0617] |
| Data/restraints/parameters | 18,597/126/1297 | 17,005/0/1342 |
| Goodness-of-fit on $F^2$ | 1.029 | 1.032 |
| Final $R$ indices [$I > 2\sigma(I)$] | $R_1 = 0.0722$, $wR_2 = 0.1761$ | $R_1 = 0.0506$, $wR_2 = 0.1262$ |
| $R$ indices (all data) | $R_1 = 0.1076$, $wR_2 = 0.1928$ | $R_1 = 0.0650$, $wR_2 = 0.1353$ |



### 2.4. *X-ray structure determination*

A single crystal was carefully selected under an optical microscope and glued at the tip of a thin glass fiber with cyanoacrylate adhesive. X-ray diffraction data were collected on a Bruker APEX-II CCD diffractometer at 296(2) K using Mo-K$\alpha$ radiation ($\lambda = 0.71073$ Å). The structure was solved by direct methods and refined by matrix least squares on $F^2$ using the SHELXTL-97 program [27]. The intensities were corrected by full-Lorentz-polarization factors and empirical absorption. All non-hydrogen atoms were refined anisotropically. Hydrogens were placed in idealized positions and refined with a riding model using default SHELXL parameters. Those hydrogens attached to lattice water were not located. The crystal data and structure refinements of **1** and **2** are summarized in table 1. Selected bond lengths and angles are listed in tables 2 and 3, respectively.

## 3. Results and discussion

### 3.1. *Synthesis*

Hydrothermal syntheses are a popular method for synthesis of metal-oxide-clusters and organic–inorganic composite materials [28]. In the hydrothermal environment, critical factors such as initial reactants, reaction time, concentration, pH, crystallization temperature, and pressure can significantly affect product composition [29]. In our case, parallel experiments reveal that the pH greatly influences the formation of **1** and **2**.

Table 2. Selected bond lengths (Å) and angles (°) for **1**.

| | | | |
|---|---|---|---|
| W3–O3 | 1.753(13) | P2–O25 | 1.517(14) |
| W3–O31 | 1.828(14) | P2–O26 | 1.530(14) |
| W3–O28 | 1.915(15) | P2–O20 | 1.580(13) |
| W3–O32 | 1.921(14) | Mn1–N3 | 2.18(2) |
| W3–O29 | 1.933(14) | Mn1–N6 | 2.22(2) |
| W3–O19 | 2.341(12) | Mn1–N2 | 2.23(2) |
| W18–O18 | 1.712(14) | Mn1–N4 | 2.24(2) |
| W18–O61 | 1.862(14) | Mn1–N1 | 2.25(2) |
| W18–O57 | 1.872(14) | Mn1–N5 | 2.271(18) |
| W18–O56 | 1.874(15) | Mn2–O3 | 2.156(14) |
| W18–O60 | 1.912(14) | Mn2–N9 | 2.18(2) |
| W18–O20 | 2.389(13) | Mn2–O18$^{\#1}$ | 2.224(15) |
| P1–O23 | 1.509(15) | Mn2–N8 | 2.23(2) |
| P1–O21 | 1.517(14) | Mn2–N7 | 2.28(2) |
| P1–O22 | 1.519(15) | Mn2–N10 | 2.28(2) |
| P1–O19 | 1.581(13) | W3–O3–Mn2 | 154.1(8) |
| P2–O24 | 1.506(14) | W18–O18–Mn2$^{\#2}$ | 153.3(8) |

Symmetry transformations used to generate equivalent atoms: #1: $x+1$, $y$, $z$; #2: $x-1$, $y$, $z$.



Table 3. Selected bond lengths (Å) and angles (°) for **2**.

| | | | |
|---|---|---|---|
| W1–O1 | 1.695(11) | Co1–N9 | 1.906(15) |
| W1–O27 | 1.878(10) | Co1–N8 | 1.916(14) |
| W1–O22 | 1.884(10) | Co1–N4 | 1.926(18) |
| W1–O19 | 1.923(11) | Co1–N12 | 1.920(15) |
| W1–O61 | 2.395(9) | Co1–N5 | 1.935(15) |
| W2–O2 | 1.690(11) | Co1–N1 | 1.938(13) |
| W2–O23 | 1.892(10) | Co2–N17 | 1.926(14) |
| W2–O19 | 1.925(11) | Co2–N24 | 1.912(12) |
| W2–O20 | 1.913(11) | Co2–N16 | 1.928(15) |
| W2–O61 | 2.366(10) | Co2–N13 | 1.923(14) |
| W17–O17 | 1.681(12) | Co2–N20 | 1.906(14) |
| W17–O48 | 1.905(10) | Co2–N21 | 1.945(14) |
| W17–O47 | 1.875(11) | N9–Co1–N4 | 174.7(6) |
| W17–O53 | 1.913(11) | N9–Co1–N8 | 89.5(6) |
| W17–O52 | 1.925(11) | N9–Co1–N5 | 93.7(6) |
| W17–O62 | 2.372(10) | N12–Co1–N5 | 174.4(6) |
| W18–O18 | 1.707(11) | N1–Co1–N4 | 82.3(7) |
| W18–O50 | 1.905(11) | N24–Co2–N17 | 92.0(5) |
| W18–O49 | 1.887(11) | N21–Co2–N17 | 93.1(6) |
| W18–O53 | 1.924(12) | N20–Co2–N21 | 174.2(6) |
| W18–O54 | 1.950(11) | N13–Co2–N16 | 83.7(6) |
| W18–O62 | 2.364(10) | N21–Co2–N24 | 82.7(5) |

The optimum pH range is 4.8–6.2. To investigate the influence of initial reactants on the formation of **1** and **2** we used $Na_2WO_4 \cdot 2H_2O$ and $H_3PO_4$ as starting materials instead of $\alpha$-$H_6P_2W_{18}O_{62} \cdot nH_2O$, no products were obtained under the same conditions, showing that $\alpha$-$H_6P_2W_{18}O_{62} \cdot nH_2O$ is necessary as a precursor to synthesize **1** and **2**. In addition, when $MnCl_2 \cdot 4H_2O$ were replaced by $MnSO_4$ and/or $Mn(OAc)_2$ **1** was not obtained. In our experiments, the presence of trea is critical for the crystallization of **1** and **2**. When trea was removed, nothing could be isolated except an orange precipitate with an IR spectrum very similar to those of **1** and **2**. So we presume that trea is beneficial for crystal growth.

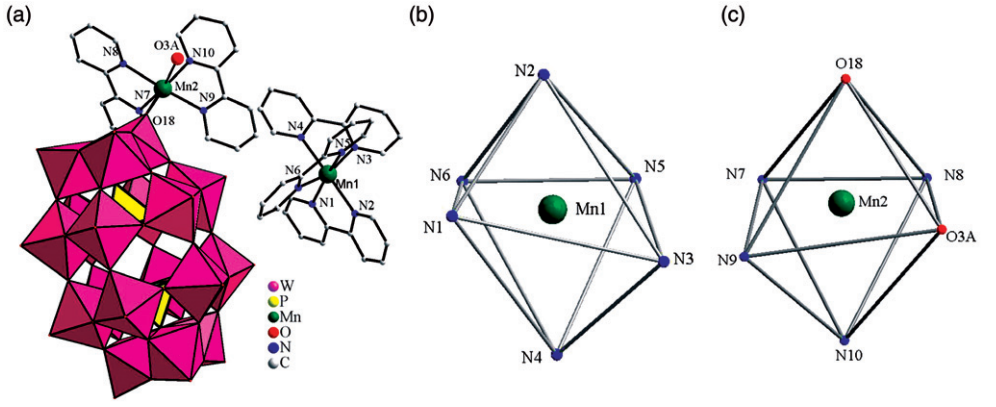


Figure 1. (a) The structural unit of **1**. All hydrogens are omitted for clarity. The atoms with suffix A are generated by the symmetry operation, A: $-1+x$, $y$, $z$. (b) Coordination geometry of $[Mn1(2,2'\text{–bipy})_3]^{2+}$ cation. (c) Coordination geometry of $[Mn2(2,2'\text{–bipy})_2]^{2+}$ cation.

### 3.2. *Crystal structures of 1 and 2*

Compounds **1** and **2** are built from the classical Dawson-type polyoxoanion $[\alpha\text{-}P_2W_{18}O_{62}]^{6-}$ and transition-metal complexes. The Dawson-type polyoxoanion $[\alpha\text{-}P_2W_{18}O_{62}]^{6-}$ is composed of two $[\alpha\text{-}PW_9O_{34}]^{3-}$ units derived from $[\alpha\text{-}PW_{12}O_{40}]^{3-}$ by removal of three corner-shared $WO_6$ octahedra, and fused into a cluster of virtual $D_{3h}$ symmetry. In **1** and **2**, the W–O distances can be grouped into four sets according to the numbers and types of oxygen atoms: (1) 18 terminal oxygens bonded to one tungsten with W–O distances of 1.653(15)–1.753(13) Å for **1** and 1.674(12)–1.722(11) Å for **2**. (2) 36 bridging oxygens which are shared by two tungstens with W–O distances of 1.828(14)–1.989(14) Å for **1** and 1.852(10)–1.950(11) Å for **2**. (3) Six bridging oxygens which are combined with one phosphorus and two tungstens with W–O distances of 2.333(14)–2.403(15) Å for **1** and 2.343(9)–2.392(10) Å for **2**. (4) two bridging oxygens which are coordinated to one phosphorus and three tungstens with W–O distances of 2.341(12)–2.410(14) Å for **1** and 2.364(10)–2.395(9) Å for **2**, within the normal ranges [13, 14]. Corresponding P–O distances are in the range 1.506(14)–1.581(13) Å, 1.510(10)–1.580(10) Å, respectively, within normal ranges and close to those described in $H_2[Ca_2(P_2W_{18}O_{62})(H_2O)_5]\cdot 7.5H_2O$, $[Zn(phen)_2(ppy)][\{Zn(phen)_2\}\{Zn(phen)_2(H_2O)\}\cdot\{P_2W_{18}O_{62}\}]\cdot 2H_2O$ (ppy = 2-(5-phenylpyridin-2-yl)pyridine) and $[Cu(phen)_3][Cu(phen)_2Cu(phen)_2(P_2W_{18}O_{62})]\cdot 2H_2O$ [23, 30, 31].

Compound **1** is a 1-D infinite chain based on $[P_2W_{18}O_{62}]^{6-}$ and $[Mn(2,2'\text{-bipy})_2]^{2+}$ linkers. Single crystal X-ray diffraction analysis reveals that the structural unit of **1** is constructed from one $[Mn(2,2'\text{-bipy})_3]^{2+}$, two protons, and one $[Mn(2,2'\text{-bipy})_2(P_2W_{18}O_{62})]^{4-}$. Considering the charge balance requirement of $[Mn(2,2'\text{-bipy})_2(P_2W_{18}O_{62})]^{4-}$ along with one $[Mn(2,2'\text{-bipy})_2]^{2+}$, two $H^+$ ions are needed, consistent with the acidic environment of the reaction system. To localize the possible positions of two protons, the bond valence sum (BVS) calculations of all oxygens in **1** have been performed. Although they cannot be accurately located by X-ray diffraction and BVS calculations, these protons must be in $[P_2W_{18}O_{62}]^{6-}$ [32]; the molecular formula of **1** can be defined as $[Mn(2,2'\text{-bipy})_3]H_2[Mn(2,2'\text{-bipy})_2][P_2W_{18}O_{62}]$. As shown in figure 1(a), the $[Mn(2,2'\text{-bipy})_2(P_2W_{18}O_{62})]^{4-}$ polyoxoanion is formed

Figure 2. Combined polyhedral/ball-and-stick representation of the 1-D chain in **1**.

by a $[Mn(2,2'\text{-bipy})_2]^{2+}$ cation coordinating to a terminal oxygen of a "cap" $WO_6$ octahedron of $[P_2W_{18}O_{62}]^{6-}$ through the Mn(2)–O–W bridge. Adjacent $[Mn(2,2'\text{-bipy})_2(P_2W_{18}O_{62})]^{4-}$ polyoxoanions alternately connect each other through the terminal oxygens (O3 and O18) located in the "cap" site of Dawson-type polyoxoanions, leading to a 1-D zigzag chain structure in –ABABAB– mode (figure 2). Metal–organic cations connecting neighboring Dawson-type polyoxoanions through terminal oxygens located in the "cap" sites of polyoxoanions is rare [33]. In most cases, terminal oxygens located in the "belt" sites of Dawson-type polyoxoanions coordinate metal cations connecting neighboring polyoxoanions [13, 14, 16, 20].

There are two crystallographically unique $Mn^{2+}$ cations ($[Mn1(2,2'\text{-bipy})_3]^{2+}$ and $[Mn2(2,2'\text{-bipy})_2]^{2+}$) in **1**. As shown in figure 1(b), the $[Mn1(2,2'\text{-bipy})_3]^{2+}$ is six-coordinate octahedral. Dihedral angles among the three 2,2′-bipy planes are 82.45°, 83.078°, and 89.79°, indicating that 2,2′-bipy are not perpendicular. The $[Mn2(2,2'\text{-bipy})_2]^{2+}$ is also octahedral with the equatorial plane formed by a terminal oxygen (O18) from a $[P_2W_{18}O_{62}]^{6-}$ (Mn–O: 2.156(14) Å) and three nitrogens (N7, N8, and N9) from two 2,2′-bipy ligands (Mn–N: 2.18(2)–2.28(2) Å); a terminal oxygen (O3A, A: $-1+x, y, z$) from $[P_2W_{18}O_{62}]^{6-}$ (Mn–O: 2.224(15) Å) and a nitrogen (N10) from 2,2′-bipy occupy the apical sites (Mn–N: 2.28(2) Å) (figure 1c).

Compound **2** consists of a discrete $[\alpha\text{-}P_2W_{18}O_{62}]^{6-}$ cluster, two $[Co(H_2biim)_3)]^{2+}$ cations and eight lattice waters (figure 3). Each $[Co(H_2biim)_3)]^{2+}$ is six-coordinate octahedral with Co–N distances of 1.906(14)–1.945(14) Å (average 1.92 Å). Dihedral angles among three $H_2$biim planes in the $[Co1(H_2biim)_3)]^{2+}$ cation are 81.95°, 85.58°, and 86.10°, respectively, and dihedral angles among three $H_2$biim planes in the $[Co2(H_2biim)_3)]^{2+}$ cation are 81.80°, 84.20°, and 86.44°, respectively, indicating that $[Co1(H_2biim)_3)]^{2+}$ and $[Co2(H_2biim)_3)]^{2+}$ are distorted.

Design and assembly of supramolecular architectures are of interest in supramolecular chemistry and crystal engineering because they can construct spectacular topologies and functional materials [34–36]. As attractive inorganic building blocks, POMs have played a substantial role in this filed [37, 38]. Supramolecular architectures are present in **1** and **2**. As shown in figure 4(a), adjacent chains in **1** are linked into a 3-D supramolecular framework through edge-to-face aromatic C–H$\cdots\pi$ interactions with C(39)$\cdots\pi$ separation of 3.5 Å and the C(39)–H(39)$\cdots\pi$ angle of 148.5° and face-to-face $\pi$–$\pi$ stacking interactions between neighboring 2,2′-bipy rings along *a*-axis. The supramolecular structure of **2** (figure 4b) is generated by hydrogen-bonding interactions (table 4) between nitrogens of $H_2$biim ligands and surface oxygens of polyoxoanions and water as well as C–H$\cdots\pi$ interactions with C(30)$\cdots\pi$ separation of 3.7 Å and the C(30)–H(30)$\cdots\pi$ angle of 117.7°. Obviously, supramolecular interactions are responsible for the chemical stability of **1** and **2**. Similar 3-D extended supramolecular

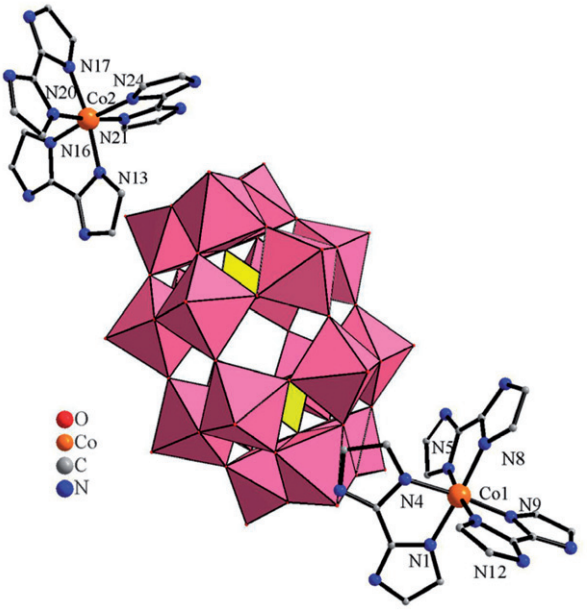


Figure 3. The structural unit of **2**. All hydrogens and waters are omitted for clarity.

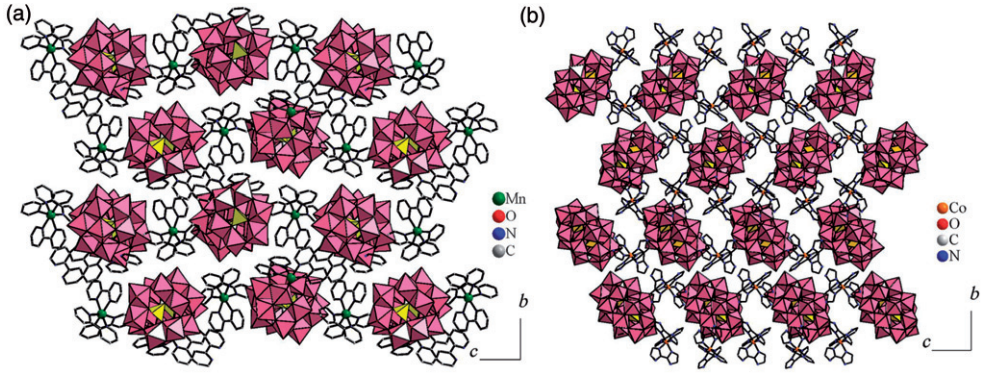


Figure 4. (a) Combined polyhedral/ball-and-stick representation of the 3-D supramolecular structure in **1**. (b) Combined polyhedral/ball-and-stick representation of the 3-D supramolecular structure in **2**. All hydrogens and waters are omitted for clarity.

architectures have been observed in Dawson-based polyoxotungstates $[Zn(phen)_2(ppy)][\{Zn(phen)_2\}\{Zn(phen)_2(H_2O)\}\cdot\{P_2W_{18}O_{62}\}]\cdot 2H_2O$ and $[Cu(phen)_3][Cu(phen)_2Cu(phen)_2(P_2W_{18}O_{62})]\cdot 2H_2O$ [30, 31].

### 3.3. *FT-IR spectra, thermal analyses and XPS spectra*

IR spectra (Supplementary material) of **1** and **2** display four characteristic vibration patterns of the Dawson-type polyoxoanion, assigned to $\nu$(P–O), $\nu$(W–$O_t$) (terminal oxygen), $\nu$(W–$O_b$–W) (corner-sharing oxygen), and $\nu$(W–$O_c$–W) (edge-sharing oxygen)

Table 4. Hydrogen bond lengths (Å) and bond angles (°) for **2**.

| D–H | A | D–H | H···A | D–H–A | D···A | Symmetry code |
|---|---|---|---|---|---|---|
| N2–H2B | O8W | 0.860 | 1.843 | 160.71 | 2.670 | |
| N3–H3A | O7W | 0.860 | 1.889 | 152.91 | 2.684 | |
| N6–H6B | O15 | 0.860 | 2.013 | 169.63 | 2.863 | $x+1, y, z$ |
| N7–H7B | O44 | 0.860 | 1.955 | 163.97 | 2.792 | $x+1, y, z$ |
| N10–H10A | O3W | 0.860 | 2.188 | 135.48 | 2.865 | |
| N11–H11B | O3W | 0.860 | 2.129 | 139.36 | 2.837 | |
| N11–H11B | O4 | 0.860 | 2.286 | 123.10 | 2.848 | $x+1, -y+1/2, z-1/2$ |
| N14–H14B | O1W | 0.860 | 1.893 | 158.16 | 2.711 | |
| N15–H15A | O42 | 0.860 | 2.103 | 136.77 | 2.793 | $x-1, y, z$ |
| N18–H18B | O5W | 0.860 | 2.052 | 149.68 | 2.828 | $x, y, z-1$ |
| N19–H19B | O5W | 0.860 | 2.344 | 141.29 | 3.063 | $x, y, z-1$ |
| N22–H22A | O2W | 0.860 | 2.015 | 148.21 | 2.783 | |
| N22–H22A | O12 | 0.860 | 2.615 | 114.93 | 3.078 | $-x+2, -y, -z+1$ |
| N23–H23B | O2W | 0.860 | 2.482 | 136.18 | 3.159 | |



at 1089, 959, 910, and 789–755 $cm^{-1}$ for **1**; 1090, 960, 912, and 788–755 $cm^{-1}$ for **2** [13]. Comparing IR spectra of **1** and **2** to that of $\alpha$-$H_6P_2W_{18}O_{62} \cdot nH_2O$ [13(c), 20], the P–O, W–$O_t$, and W–$O_b$–W vibration frequencies are nearly the same as $\alpha$-$H_6P_2W_{18}O_{62} \cdot nH_2O$, while the W–$O_c$–W vibration splits into two bands, indicating that the polyoxoanions in **1** and **2** retain the basic Dawson structure but with some distortion resulting from strong interactions between metal–organic cations and $[\alpha\text{-}P_2W_{18}O_{62}]^{6-}$ [13, 20]. The vibration bands between 1400 and 1600 $cm^{-1}$ correspond to stretching vibration modes of 2,2′-bipy. In comparison with free 2,2′-bipy, the absorption at 1443 $cm^{-1}$ attributable to the $\nu_{as}$(C–N of 2,2′-bipy) in **1** is red-shifted to 1434 $cm^{-1}$ from the coordination of 2,2′-bipy [39]. In **2**, $H_2$biim is a bidentate chelating ligand and both N–H groups remain protonated [40]. Vibrations at 3145, 1532, 1382, 1188 and 1140 $cm^{-1}$ are indicative of $H_2$biim [41].

Thermogravimetric (TG) curve of **1** shows one step weight loss of 14.38% in the range of 25–900°C (Supplementary material), which can be assigned to the loss of water and 2,2′-bipy (Calcd 15.20%). The TG curve of **2** exhibits a total weight loss of 17.96% in the range of 25–900°C, close to the calculated value of 17.79% (Supplementary material). The first step weight loss of 3.32% at 25–362°C corresponds to release of eight lattice and one structural water (Calcd 2.98%). The second weight loss of 14.64% at 411–750°C arises from decomposition of six $H_2$biim molecules (Calcd 14.81%).

The XPS spectra in **1** exhibit two overlapped peaks at 35.66 and 37.75 eV (Supplementary material), attributed to W4$f_{7/2}$ and W4$f_{5/2}$ of W(VI) [42(a), 42(b)] and two peaks at 641.7 and 653.6 eV assigned to Mn2$p_{3/2}$ and Mn2$p_{1/2}$ [42(c), 42(d)]. As for **2** (Supplementary material), the XPS spectra exhibit two overlapped peaks at 35.29 and 37.54 eV, corresponding to W4$f_{7/2}$ and W4$f_{5/2}$ and two peaks at 780.3 and 796.02 eV attributed to Co2$p_{3/2}$ and Co2$p_{1/2}$ [42(e), 42(f)]. All these results are in good agreement with the structural analysis.

### 3.4. *Photoluminescence properties*

Emission spectra of **1** and **2** in the solid state at room temperature are depicted in "Supplementary material." Compound **1** exhibits a broad blue photoluminescence

emission band at *ca* 438 nm upon excitation at *ca* 340 nm. The starting material $\alpha$-$H_6P_2W_{18}O_{62} \cdot nH_2O$ does not emit luminescence. Free 2,2′-bipy displays weak luminescence at 530 nm in the solid state at room temperature. Thus, the blue-shift of the luminescence of **1** compared to that of the free 2,2′-bipy ligand may be related to the coordination of the 2,2′-bipy and ligand-to-metal charge transfer (LMCT) [43–46]. Upon excitation at *ca* 361 nm, **2** in the solid state exhibits strong photoluminescence with emission maximum at 440 nm, very similar to that of the free $H_2$biim ligand with $\lambda_{em} = 423$ nm. The photoluminescence of **2** therefore results from the emission of the $H_2$biim ligand [41, 47, 48].

## 4. Conclusions

Two new organic–inorganic hybrid polyoxotungstates $[Mn(2,2'\text{-bipy})_3]H_2[Mn(2,2'\text{-bipy})_2][P_2W_{18}O_{62}]$ (**1**) and $[Co(H_2biim)_3)]_2H_2[P_2W_{18}O_{62}] \cdot 8H_2O$ (**2**) have been hydrothermally synthesized. Compound **1** exhibits a 1-D zigzag chain constructed from alternate Dawson-type heteropolyanions $[\alpha\text{-}P_2W_{18}O_{62}]^{6-}$ and $[Mn(2,2'\text{-bipy})_2]^{2+}$, while **2** is a discrete structure consisting of $[\alpha\text{-}P_2W_{18}O_{62}]^{6-}$ and two $[Co(H_2biim)_3)]^{2+}$. The syntheses of the POM derivatives demonstrates again that hydrothermal techniques are a route to new kinds of organic–inorganic hybrids. Compound **1** exhibits a broad emission band at 438 nm upon excitation at 340 nm and **2** shows strong photoluminescence with an emission at 440 nm upon excitation at 361 nm. A large class of Dawson-type POM derivatives could be obtained by introducing different TM cations, even metal carbonyl cations.



## Supplementary material

Crystallographic data for the structural analyses reported in this article have been deposited with the Cambridge Crystallographic Data Centre with CCDC nos 754608 for **1** and 754609 for **2**. Copies of this information may be obtained free of charge from the Director, CCDC, 12 Union Road, Cambridge, CB2 1EZ, UK (Fax: +44 1223 336033; Email: deposit@ccdc.cam.ac.uk).

## Acknowledgments

We thank the National Natural Science Foundation of China, the Natural Science Foundation of Henan Province and Foundation of Education Department of Henan Province for financial support.

## References

[1] F. Hussain, U. Kortz, B. Keita, L. Nadjo, M.T. Pope. *Inorg. Chem.*, **45**, 761 (2006).
[2] C.T. Kressge, M.E. Leonowicz, W.J. Roth, J.C. Vartuni, J.S. Beck. *Nature*, **359**, 710 (1992).
[3] H.Y. An, E.B. Wang, L. Xu. *Angew. Chem. Int. Ed.*, **118**, 918 (2006).

[4] L. Lisnard, A. Dolbecq, P. Mialane, J. Marrot, E. Codjovi, F. Sécheresse. *J. Chem. Soc., Dalton Trans*., 3913 (2005).
[5] M.T. Pope, T. Yamase (Eds). *Polyoxometalate Chemistry for Nanocomposite Design*, Kluwer, Dordrecht (2002).
[6] M.T. Pope, A. Müller (Eds). *Polyoxometalates: From Topology via Self-Assembly to Applications*, Kluwer, Dordrecht (2001).
[7] M.T. Pope, A. Müller (Eds). *Polyoxometalates: From Platonic Solids to Antiretroviral Activity*, Kluwer, Dordrecht (1994).
[8] E. Burkholder, V. Golub, C.J. O'Connor, J. Zubieta. *Inorg. Chem*., **42**, 6729 (2003).
[9] A. Müller, S.Q.N. Shah, H. Bögge, M. Schmidtmann. *Nature*, **397**, 48 (1999).
[10] B.B. Yan, Y. Xu, X.H. Bu, N.K. Goh, L.S. Chia, G.D. Stucky. *J. Chem. Soc., Dalton Trans*., **13**, 2009 (2001).
[11] X.L. Wang, C. Qin, E.B. Wang, Z.M. Su, Y.G. Li, L. Xu. *Angew. Chem. Int. Ed*., **45**, 7411 (2006).
[12] R.G. Cao, S.X. Liu, L.H. Xie, Y.B. Pan, J.F. Cao, Y.H. Ren, L. Xu. *Inorg. Chem*., **46**, 3541 (2007).
[13] (a) J.Y. Niu, D.J. Guo, J.W. Zhao, J.P. Wang. *New J. Chem*., **28**, 980 (2004); (b) J.Y. Niu, D.J. Guo, J.P. Wang, J.W. Zhao. *Cryst. Growth Des*., **4**, 241 (2004); (c) J.P. Wang, J.W. Zhao, J.Y. Niu. *J. Mol. Struct*., **697**, 191 (2004).
[14] H. Jin, Y.F. Qi, D.R. Xiao, X.L. Wang, S. Chang, E.B. Wang. *J. Mol. Struct*., **837**, 23 (2007).
[15] A.X. Tian, Z.G. Han, J. Peng, J.Q. Sha, J.L. Zhai, P.P. Zhang, J. Chen, H.S. Liu. *Z. Anorg. Allg. Chem*., **633**, 2730 (2007).
[16] T. Soumahoro, E. Burkholder, W. Ouellette, J. Zubieta. *Inorg. Chim. Acta*, **358**, 606 (2005).
[17] B.Z. Lin, L.W. He, B.H. Xu, X.L. Li, Z. Li, P.D. Liu. *Cryst. Growth Des*., **9**, 273 (2009).
[18] A.X. Tian, Z.G. Han, J. Peng, B.X. Dong, J.Q. Sha, B. Li. *J. Mol. Struct*., **832**, 117 (2007).
[19] A.X. Tian, J. Ying, J. Peng, J.Q. Sha, D.X. Zhu, H.J. Pang, P.P. Zhang, Y. Chen, M. Zhu. *Inorg. Chem. Commun*., **11**, 1132 (2008).
[20] J.W. Zhao, S.T. Zheng, W. Liu, G.Y. Yang. *J. Solid State Chem*., **181**, 637 (2008).
[21] J.Q. Sha, C. Wang, J. Peng, J. Chen, A.X. Tian, P.P. Zhang. *Inorg. Chem. Commun*., **10**, 1321 (2007).
[22] (a) J.Q. Sha, J. Peng, Y.Q. Lan, Z.M. Su, H.J. Pang, A.X. Tian, P.P. Zhang, M. Zhu. *Inorg. Chem*., **47**, 5145 (2008); (b) J.Q. Sha, J. Peng, Y.G. Li, P.P. Zhang, H.J. Pang. *Inorg. Chem. Commun*., **11**, 907 (2007); (c) H.J. Pang, J. Peng, J.Q. Sha, A.X. Tian, P.P. Zhang, Y. Chen, M. Zhu. *J. Mol. Struct*., **921**, 289 (2009).
[23] J.P. Wang, D. Yang, J.Y. Niu. *J. Coord. Chem*., **61**, 3651 (2008).
[24] X.Y. Zhao, D.D. Liang, S.X. Liu, C.Y. Sun, R.G. Cao, C.Y. Gao, Y.H. Ren, Z.M. Su. *Inorg. Chem*., **47**, 7133 (2008).
[25] F. Yao, F.X. Meng, Y.G. Chen, C.J. Zhang. *J. Coord. Chem*., **63**, 196 (2010).
[26] R.G. Finke, M.W. Droege, P.J. Domaille. *Inorg. Chem*., **26**, 3886 (1987).
[27] G.M. Sheldrick. *SHEXTL-97, Program for Crystal Structure Refinement*, University of Göttingen, Germany (1997).
[28] (a) M. Yuan, Y.G. Li, E.B. Wang, C.G. Tian, L. Wang, C.W. Hu, N.H. Hu, H.Q. Jia. *Inorg. Chem*., **42**, 3670 (2003); (b) P.J. Hagrman, D. Hagrman, J. Zubieta. *Angew. Chem. Int. Ed*., **38**, 2638 (1999).
[29] (a) H. Jin, Y.F. Qi, E.B. Wang, Y.G. Li, X.L. Wang, C. Qin, S. Chang. *Cryst. Growth Des*., **6**, 2693 (2006); (b) K. Pavani, S.E. Lofland, K.V. Ramanujachary, A. Ramanan. *Eur. J. Inorg. Chem*., 3080 (2005).
[30] A.X. Tian, Z.G. Han, J. Peng, J.L. Zhai, B.X. Dong, J.Q. Sha. *J. Coord. Chem*., **60**, 1645 (2007).
[31] J. Wang, F.B. Li, L.H. Tian, S.Y. Cheng. *J. Coord. Chem*., **61**, 2122 (2008).
[32] J.Y. Niu, P.T. Ma, H.Y. Niu, J. Li, J.W. Zhao, Y. Song, J.P. Wang. *Chem. Eur. J*., **13**, 8739 (2007).
[33] H.X. Yang, J.X. Lin, J.T. Chen, X.D. Zhu, S.Y. Gao, R. Cao. *Cryst. Growth Des*., **8**, 2623 (2008).
[34] B. Moulton, M.J. Zaworotko. *Chem. Rev*., **101**, 1629 (2001).
[35] O.M. Yaghi, M. O'Keeffe, N.W. Ockwig, H.K. Chae, M. Eddaoudi, J. Kim. *Nature*, **423**, 705 (2003).
[36] J.W. Zhao, S.T. Zheng, G.Y. Yang. *J. Solid State Chem*., **181**, 2205 (2008).
[37] R. Atencio, A. Briceño, X. Galindo. *Chem. Commun*., **5**, 637 (2005).
[38] P.Q. Zheng, Y.P. Ren, L.S. Long, R.B. Huang, L.S. Zheng. *Inorg. Chem*., **44**, 1190 (2005).
[39] M.I. Khan, E. Yohannes, S. Ayesh, R.J. Doedens. *J. Mol. Struct*., **656**, 45 (2003).
[40] L.M. Gruia, F.D. Rochon, A.L. Beauchamp. *Inorg. Chim. Acta*, **360**, 1825 (2007).
[41] R.L. Sang, L. Xu. *Polyhedron*, **25**, 2167 (2006).
[42] (a) Z.H. Yi, X.B. Cui, X. Zhang, Y. Chen, J.Q. Xu, G.D. Yang, Y.B. Liu, X.Y. Yu, H.H. Yu, W.J. Duan. *Inorg. Chem. Commun*., **10**, 1448 (2007); (b) J.P. Wang, P.T. Ma, J.W. Zhao, J.Y. Niu. *Inorg. Chem. Commun*., **10**, 523 (2007); (c) F.T. Xie, L.M. Duan, X.Y. Chen, P. Cheng, J.Q. Xu, H. Ding, T.G. Wang. *Inorg. Chem. Commun*., **8**, 274 (2005); (d) T. Qin, J. Lu, S. Wei, P.F. Qi, Y.Y. Peng, Z.P. Yang, Y.T. Qian. *Inorg. Chem. Commun*., **5**, 369 (2002); (e) G.G. Gao, L. Xu, W.J. Wang, X.S. Qu, H. Liu, Y.Y. Yang. *Inorg. Chem*., **47**, 2325 (2008); (f) D.R. Xiao, E.B. Wang, H.Y. An, L. Xu, C.W. Hu. *J. Mol. Struct*., **707**, 77 (2004).
[43] L.Y. Zhang, G.F. Liu, S.L. Zheng, B.H. Ye, X.M. Zhang, X.M. Chen. *Eur. J. Inorg. Chem*., 2965 (2003).

[44] C. Qin, X.L. Wang, E.B. Wang, Y.F. Qi, H. Jin, S. Chang, L. Xu. *J. Mol. Struct.*, **749**, 138 (2005).
[45] G. Qian, M. Wang. *Mater. Lett.*, **56**, 71 (2002).
[46] N. Hao, E.H. Shen, Y.G. Li, E.B. Wang, C.W. Hu, L. Xu. *Eur. J. Inorg. Chem.*, 4102 (2004).
[47] R.L. Sang, L. Xu. *Inorg. Chim. Acta*, **359**, 525 (2006).
[48] S. Hu, A.J. Zhou, Y.H. Zhang, S. Ding, M.L. Tong. *Cryst. Growth Des.*, **6**, 2543 (2006).